Digital Discovery

PAPER

Cite this: DOI: 00.0000/xxxxxxxxxx

SLAB: Simultaneous Labeling And Binding affinity prediction for protein-ligand structures†

Aditya Ranganath,[a] Hyojin Kim,[a] Heesung Shim,[b] and Jonathan E. Allen.[c]

Received Date
Accepted Date

DOI: 00.0000/xxxxxxxxxx

Machine learning models are often used as scoring functions to predict the binding affinity of a protein-ligand complex. These models are trained with limited amounts of data with experimentally measured binding affinity values. A large number of compounds are labeled inactive through single-concentration screens without measuring binding affinities. These inactive compounds, along with the active ones, can be used to train binary classification models, while regression models are trained using compounds with binding affinities only. However, the classification and regression tasks are often handled separately, without sharing the learned feature representations. In this paper, we propose a novel model architecture that jointly performs regression and classification objectives, aiming to maximize data utilization and improve predictive performance by leveraging two complementary tasks. In our setup, the regression yields the binding affinity, whereas the classification task yields the label as active or inactive. We demonstrate our method using PDBbind, the standard 3D structure database, as well as a dataset of flavivirus protease compounds with binding affinity data. Our experiments show that the new joint training strategy improves the accuracy of the model, increasing applicability in various practical drug screening scenarios.

Contents

A Results on dengue and zika

B Dengue results for various thresholds

In order to be rigorous, we have conducted an exhaustive set of experiments for a varying set of values for IT and IA. The results are shown in appendix B, appendix B. We also present the scatter-plots in fig. 5 and fig. 4. In fig. 5 and fig. fig. 4, each row shows an increasing value of IT from 0 to 4. Similarly, each column represents the values between 2 and 5. The difference between fig. 5 and fig. 4 lies in the assignment values of the inactive complexes - In fig. 4, the inactive assignment are not strictly re-assigned. This means, a complex is assigned an inactive assignment only if the binding affinity is 0 or unassigned. In fig. 5, the inactive com-

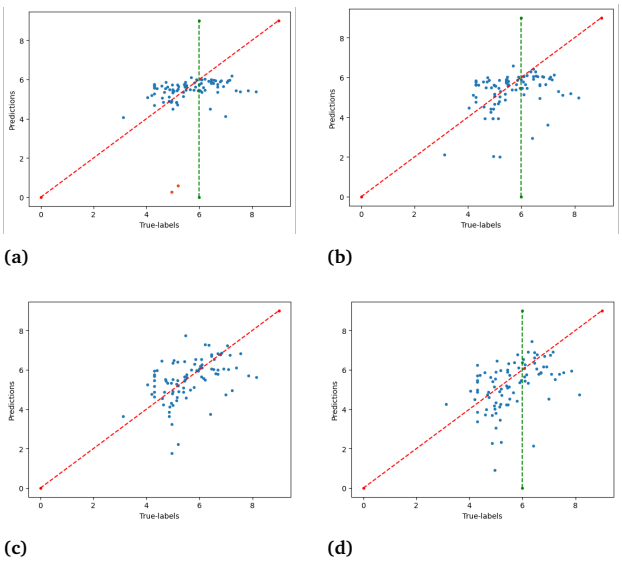

Fig. 1 The figure presents the scatter plots of Binding affinity prediction for zika. (a) represents the SGNN-SLAB results, (b) SGNN results, (c) represents EGNN-SLAB results and (d) represents the EGNN results. From the figure, and the metrics from table 1, the proposed approach with the EGNN network module outperforms the all other approaches.

[a] *Center for Applied Scientific Computing, Lawrence Livermore National Laboratory, 7000 East Avenue, Livermore, California; E-mail: ranganath2@llnl.gov*
[b] *Biosciences and Biotechnology Division, Lawrence Livermore National Laboratory, 7000 East Avenue, Livermore, California, 94550*
[c] *Global Security, Lawrence Livermore National Laboratory, 7000 East Avenue, Livermore, California, 94550*

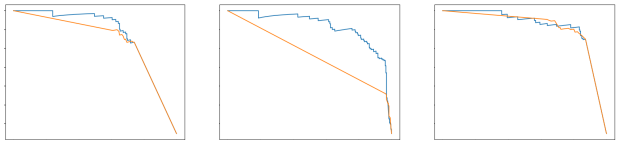

Fig. 2 Binding affinity precision recall curves for different Inactive assignments.

plexes are assigned inactive assignment values if they fall below the threshold (IT). From all these results, it is clear that the proposed SLAB architecture is able to outperform the regression-only model.

We present the training response of the cross-entropy loss in appendix B. From the figure, it is clear that the cross-entropy loss is monotonically decreasing. We also provide the loss response of the RMSE and the total loss response.

C Results on Sars-CoV-2

We present the results on Sars-CoV-2 in appendix C, and appendix C. From the figure and table, it is clear that the proposed EGNN-SLAB framework outperforms against the EGNN approach.

Approach	RMSE	MAE	r^2	Pearson (R)	Spearman (ρ)	Accuracy (%)
IT^2 IA^0	1.8322	1.4609	0.5036	0.7175	0.6790	71.26
IT^3 IA^0	1.8190	1.3194	0.5107	0.7413	0.7049	72.22
IT^4 IA^0	1.7141	1.2424	0.5655	0.7644	0.7191	84.00
IT^5 IA^0	1.7540	1.2775	0.5451	0.7537	0.7092	86.10
IT^2 IA^1	1.4753	1.1425	0.5302	0.7549	0.7107	65.17
IT^3 IA^1	1.4790	1.1330	0.5279	0.7486	0.7077	70.56
IT^4 IA^1	1.4380	1.0828	0.5537	0.7554	0.7157	85.72
IT^5 IA^1	1.4798	1.1323	0.5274	0.7390	0.7125	71.74
IT^2 IA^2	1.0805	0.8254	0.6034	0.7818	0.7545	86.58
IT^3 IA^2	1.1478	0.8839	0.5525	0.7550	0.7331	84.56
IT^4 IA^2	1.1139	0.8499	0.5786	0.7741	0.7438	84.0
IT^5 IA^2	1.1976	0.9164	0.5128	0.7430	0.7094	78.88
IT^2 IA^3	0.8865	0.6929	0.5363	0.7478	0.7393	84.63
IT^3 IA^3	0.8921	0.6558	0.5305	0.7572	0.7495	86.39
IT^4 IA^3	0.8682	0.6607	0.5552	0.7729	0.7633	86.58
IT^5 IA^3	0.8877	0.6777	0.5351	0.7418	0.7330	82.89
IT^2 IA^4	0.7078	0.5211	0.4340	0.6748	0.6977	85.62
IT^3 IA^4	0.7061	0.5016	0.4368	0.6997	0.6989	81.58
IT^4 IA^4	0.7679	0.5504	0.3339	0.6487	0.6471	85.92
IT^5 IA^4	0.7087	0.5341	0.4326	0.6802	0.7093	85.32

Table 1 The table represents all the setting used for the Inactive thresholds and the inactive affinity assignments. In these sets of experiments, we chose a loose assignment - meaning we only assigned the binding affinity value of IA to complexes with no experimentally determined binding affinity value.

Approach	RMSE	MAE	r^2	Pearson (R)	Spearman (ρ)	Accuracy (%)
IT^2 IA^0	1.5638	1.1290	0.6384	0.8040	0.7674	86.36
IT^3 IA^0	1.6603	1.2263	0.5923	0.7803	0.7444	85.63
IT^4 IA^0	1.9412	1.5078	0.4788	0.7106	0.6733	65.36
IT^5 IA^0	2.5063	1.9050	0.2611	0.5590	0.5781	65.16
IT^2 IA^1	1.5343	1.1322	0.4919	0.7322	0.6932	81.02
IT^3 IA^1	1.4676	1.0659	0.5351	0.7620	0.7358	87.46
IT^4 IA^1	1.4299	1.1113	0.5864	0.7674	0.7419	78.13
IT^5 IA^1	2.0815	1.5560	0.2656	0.5854	0.6054	74.39
IT^2 IA^2	1.1134	0.8456	0.5790	0.7853	0.7517	86.10
IT^3 IA^2	1.1481	0.8309	0.5523	0.7556	0.7400	85.02
IT^4 IA^2	1.2574	0.9488	0.4933	0.7199	0.7042	77.06
IT^5 IA^2	1.6129	1.2456	0.3121	0.5766	0.5604	73.18
IT^2 IA^3	0.8731	0.6626	0.5502	0.7498	0.7428	83.59
IT^3 IA^3	0.9673	0.7181	0.4479	0.7164	0.7108	86.26
IT^4 IA^3	0.8969	0.6646	0.5431	0.7426	0.7285	84.89
IT^5 IA^3	1.2425	0.9438	0.2810	0.5693	0.5607	72.12
IT^2 IA^4	0.6568	0.4798	0.5126	0.7222	0.7488	85.70
IT^3 IA^4	0.7122	0.5179	0.4270	0.6651	0.6696	75.72
IT^4 IA^4	0.7296	0.5365	0.3841	0.6426	0.6524	83.08
IT^5 IA^4	0.7225	0.5430	0.3960	0.6542	0.6990	79.25

Table 2 The table represents all the setting used for the Inactive thresholds and the inactive affinity assignments. In these sets of experiments, we chose a strict assignment - meaning we assigned IA to complexes with no binding affinity assigned to it and to the complexes with experimentally assigned binding affinity value if it falls below the threshold IT.

Experiments	RMSE	MAE	r^2	Pearson (R)	Spearman (ρ)	Accuracy (%)
EXP - 1	1.6387	1.1807	0.6029	0.7812	0.7465	86.08
EXP - 2	1.6383	1.2253	0.6031	0.7906	0.7497	85.31
EXP - 3	1.7391	1.2929	0.5527	0.7739	0.7302	86.36
EXP - 4	1.9519	1.5641	0.4366	0.7519	0.6987	78.27
EXP - 5	1.6710	1.2104	0.5871	0.7829	0.7387	85.77
EXP - 6	1.6410	1.2398	0.6018	0.7911	0.7415	87.32
EXP - 7	1.7894	1.3008	0.5265	0.7361	0.7058	81.11
EXP - 8	2.0815	1.5560	0.2656	0.5854	0.6054	74.39
Mean (μ)± std (σ^2)	1.7688 ± 0.1551	1.3212 ±	0.5220 ± 0.1105	0.7491 ± 0.0644	0.7145 ± 0.0447	83.0762 ± 4.3657

Table 3 The table represents the metrics for 8 different experiments using different parameter initializations for the model. Through these experiments, we are demonstrating that the method is fairly robust against all model initializations.

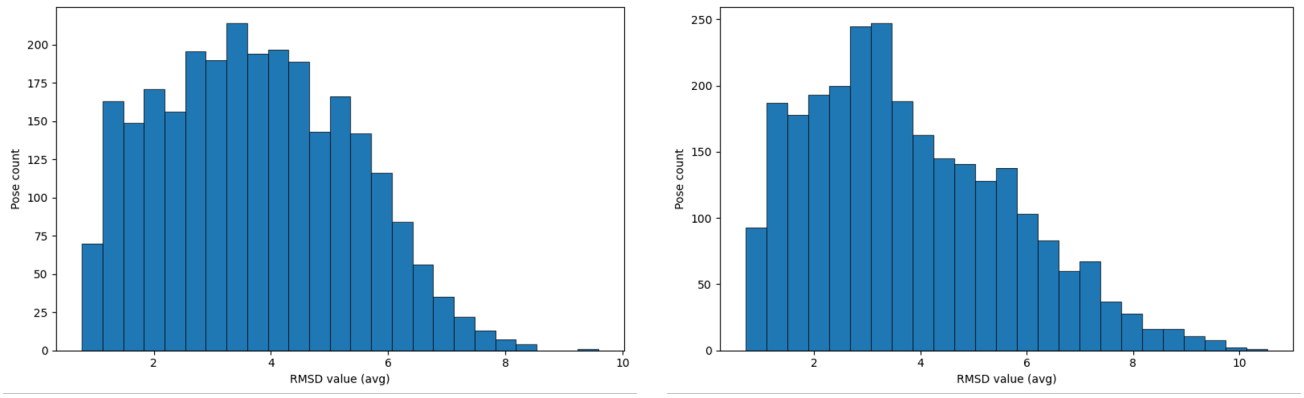

(a) (b)

Fig. 3 The figure presents the average pose RMSD from the each other. The x-axis represents the RMSD value range in , while the y-axis represents the number of poses with that count. Fig. (a) represents the pose count for Zika, while Fig. (b) presents the pose count for dengue.

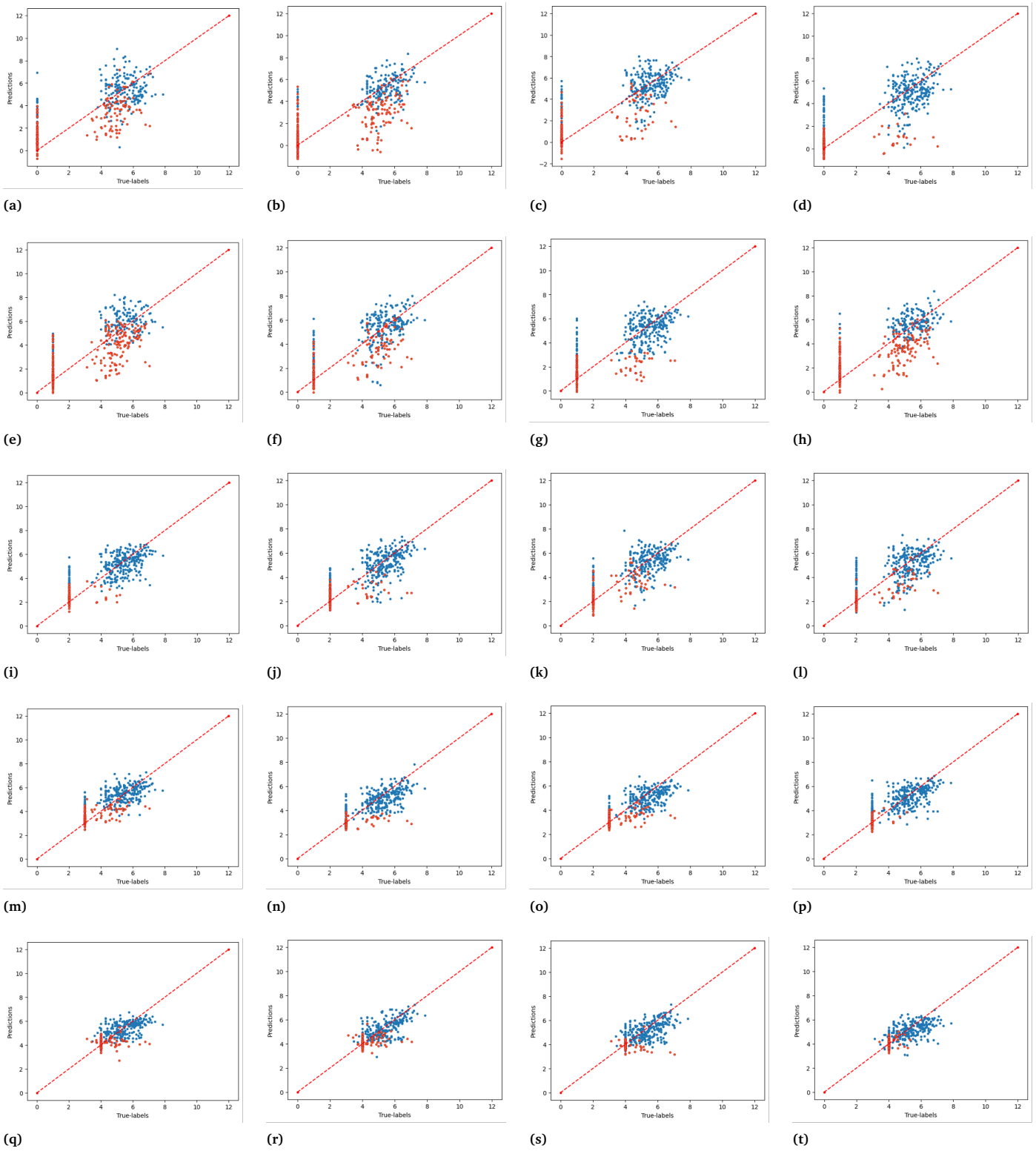

Fig. 4 The figure presents the binding affinity prediction results for dengue type-2 without a strict upper bound on the binding affinity. In these experiments, only if the binding affinity value for the complex is unassigned ($y = 0$), we assign the complex with IA, otherwise, we use the assigned value.

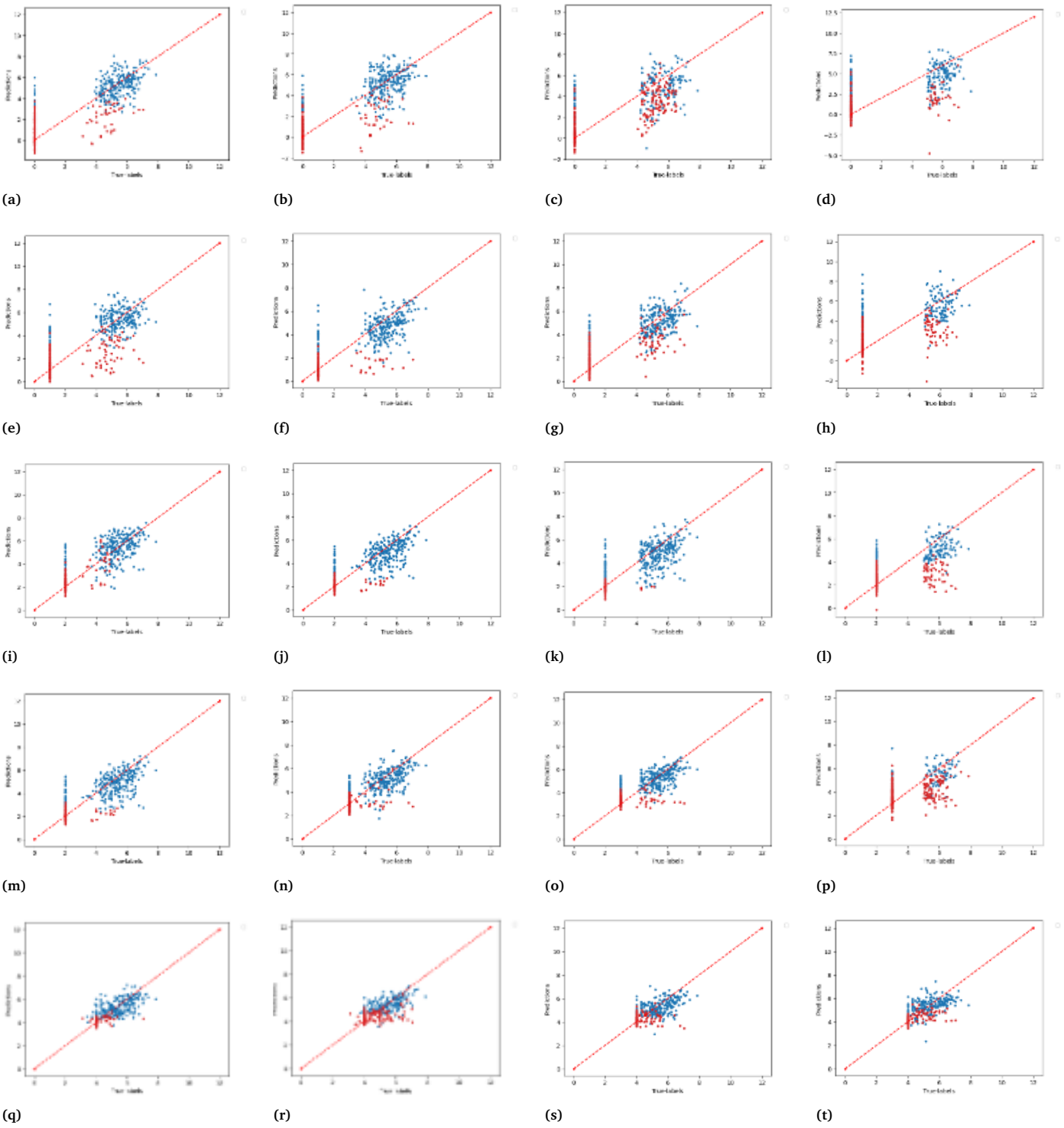

Fig. 5 The figure presents the scatter plots of binding affinity prediction for dengue type-2 with a strict upper bound. Each column represents the inactive assignment of In these experiments, we assign the inactive assignment (IA) to all complexes below the inactive threshold (IT).

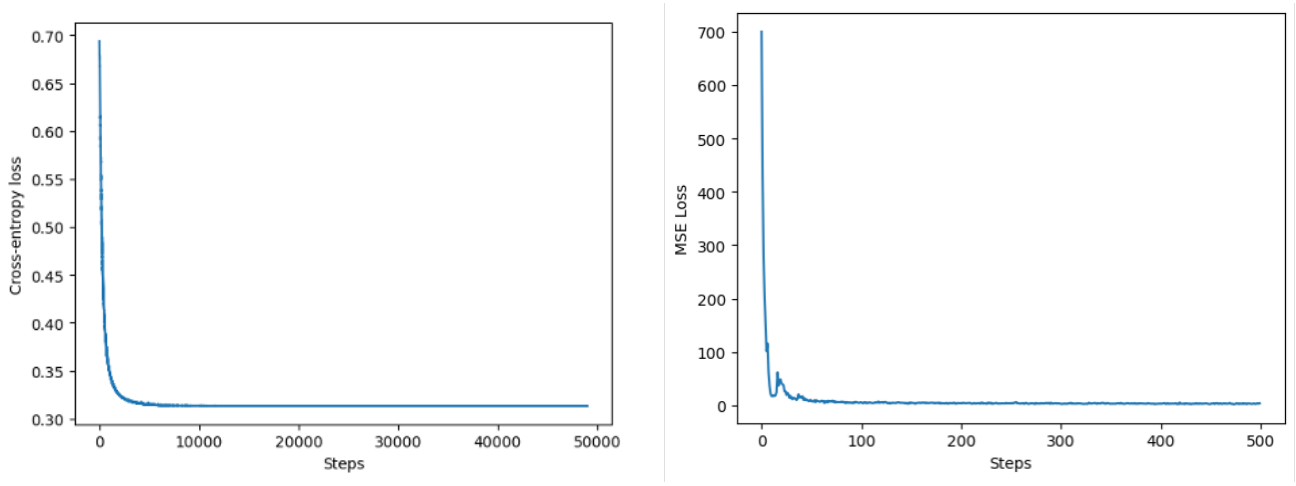

(a) (b)

Fig. 6 The figure shows the training response for the both the MSE loss and the cross-entropy loss. To avoid the loss of too much information, for the MSE loss, we present the results for the first 500 steps.

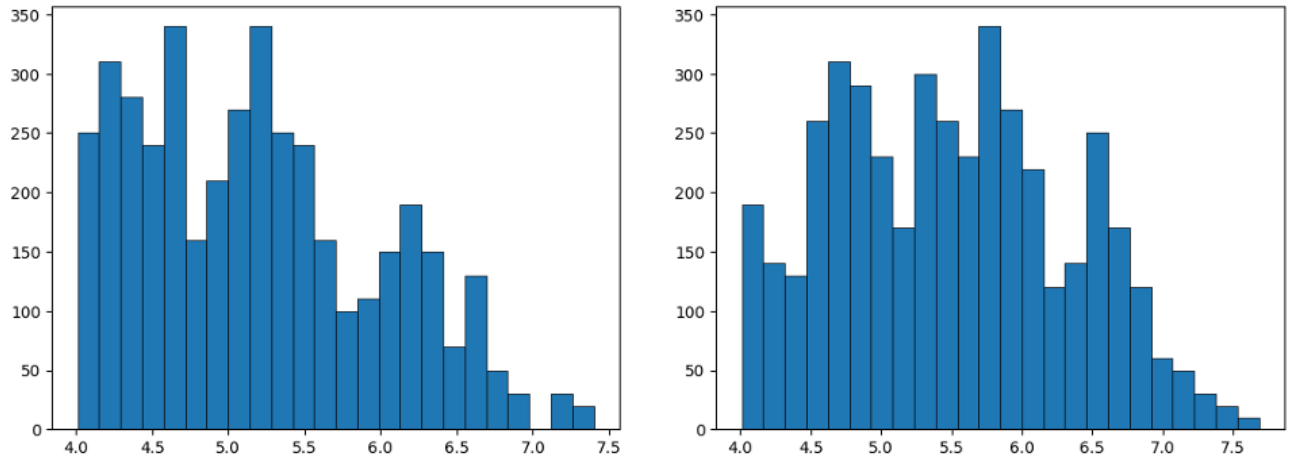

(a) (b)

Fig. 7 Distribution of train and test set of Sars-CoV-2 dataset. x-axis represents binding affinity-values and the y-axis represents the count of samples.

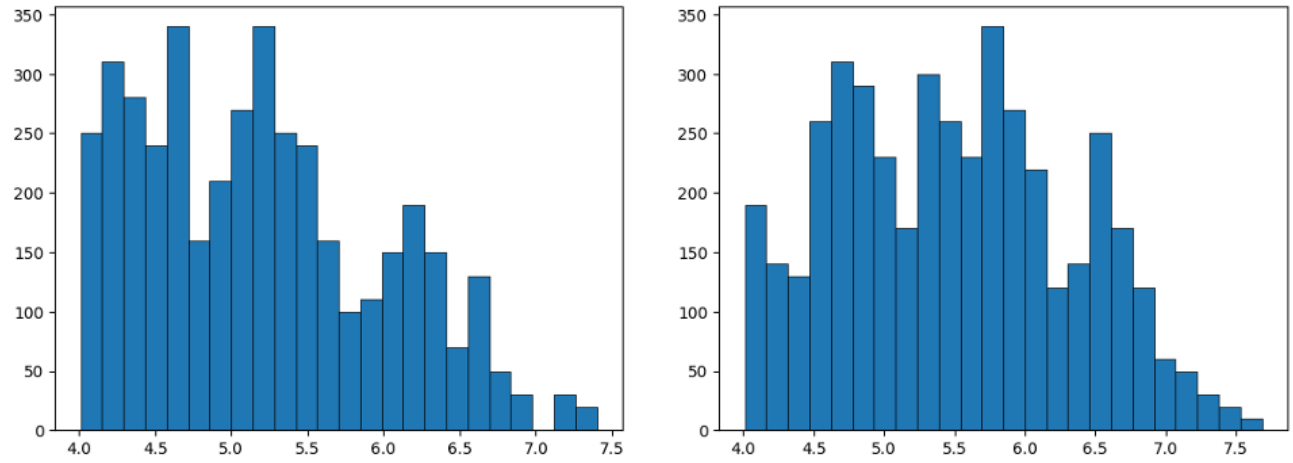

(a) (b)

Fig. 8 Distribution of train and test set of Sars-CoV-2 dataset. x-axis represents binding affinity-values and the y-axis represents the count of samples.

Experiments	Accuracy (%)	Accuracy (SLAB) (%)
EXP-1	82.53	87.32
EXP-2	80.0	86.36
EXP-3	79.24	86.08
EXP-4	78.98	85.77
EXP-5	76.70	85.31
EXP-6	76.45	81.11
EXP-7	76.43	78.27
EXP-8	71.89	74.39
Mean (μ)$\pm$ std (σ^2)	77.78 ± 2.96	83.0762 ± 4.3657

Table 4 We perform 8 experiments for a classification only model. From all these 8 experiments, and the average classification accuracy, it is clear that the proposed SLAB approach is able to achieve a higher accuracy, compared to the classification-only model. In addition, the SLAB architecture, in comparison the regression only model (see table 1 in main section), was able outperform across all metrics. This experiment shows that a classification-only model or a regression-only model is not able to match the performance of a SLAB framework and often performs worse in its predictive capability.

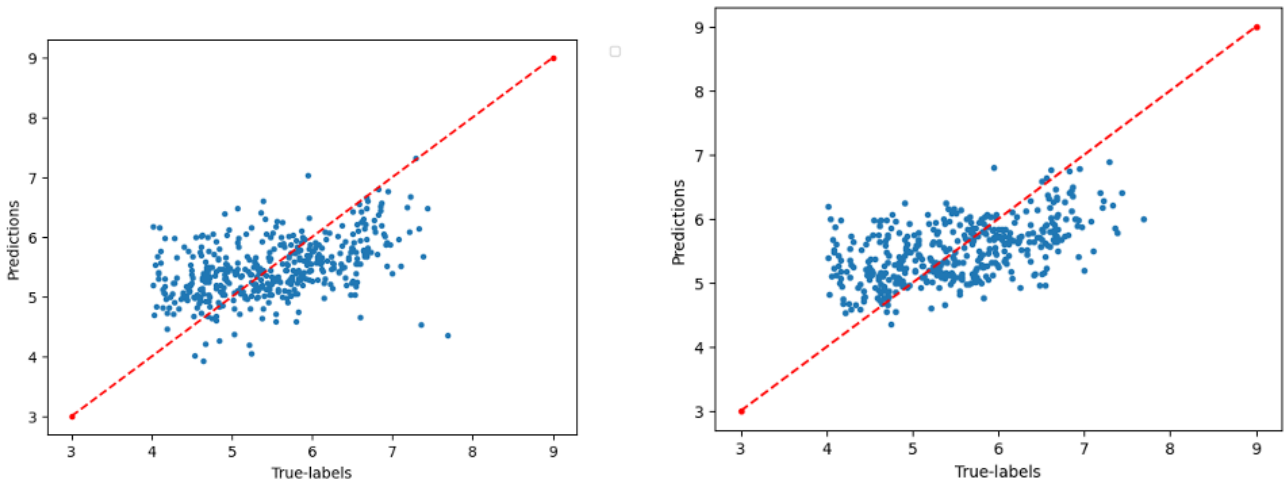

(a) (b)

Table 5 The figure shows the results on the Sars-CoV-2 dataset. The metrics are presented in table 6. Fig. (a) shows the results using SLAB architecture, while fig. (b) presents the scatter plot without using SLAB architecture.

Approach	RMSE	MAE	r^2	Pearson (R)	Spearman (ρ)
EGNN	0.7422	0.6018	0.1736	0.4501	0.4522
EGNN-SLAB	**0.7416**	**0.5966**	**0.1879**	**0.4568**	**0.4669**

Table 6 The table shows the performance of EGNN and EGNN-SLAB on the Sars-CoV-2 (Mpro) dataset. From the results, it is clear that the proposed SLAB approach is able to outperform the EGNN model.